## Supplementary Methods

### Deletion of DnaA-box clusters using a marker-free gene disruption method

To delete DnaA-box clusters from the *B. subtilis* chromosome, we developed a method for marker-free gene disruption using three steps, which was originally employed to disrupt genes in *Escherichia coli* (1,2). The steps are replacement of the target sequence with an antibiotic-resistance cassette flanked by FRT (FLP recognition target) sequences; elimination of the cassette using a helper plasmid expressing FLP recombinase; and, removal of the helper plasmid.

To construct plasmids harboring antibiotic-resistance cassettes flanked by FRT, a chloramphenicol-resistance cassette (*cat*) was amplified from the pDL2 plasmid (3) using pMB0033 and pMB0034 primers with FRT sequences and *Eco*RI or *Bam*HI recognition sites. Similarly, a spectinomycin-resistance cassette (*spec*) was amplified from the pJL62 plasmid (4) using pMB0035 and pMB0036 primers. PCR products were digested with *Eco*RI/*Bam*HI and cloned into the pMW118 plasmid (Nippon Gene Co., Ltd.), to obtain pMW118FRT-Cm and pMW118FRT-Spc, respectively.

To construct a helper plasmid expressing FLP recombinase in *B. subtilis,* the FLP gene was amplified from the pCP20 plasmid (1) using pMB0029 and pMB0030 primers harboring *Bam*HI recognition sites, and the *Bam*HI-digested PCR product was cloned into pCHE11 (5), a derivative of pBR322 containing a temperature-sensitive replication system derived from the *B. subtilis* pUB110ts-2 plasmid, to obtain pCHE11FLP.

To delete sequences harboring DnaA-Box clusters from the *B. subtilis* chromosome, *cat* or *spec* cassettes flanked by FRT sequences were amplified from pMW118FRT-Cm or pMW118FRT-Spc using pMB0065 and pMB0066 primers.

Approximately 500 bp lengths of upstream and downstream sequences of each target region were amplified from the wild-type 168 chromosome using primers indicated by F1 and R1 descriptors for the upstream regions and F2 and R2 for downstream sequences, respectively, in Table S3. The R1 and F2 primers contained sequences complementary to the FRT-F and FRT-R primers, respectively, and the three PCR products were ligated by recombinant PCR using the most widely separated primers, F1 and R2. The resulting fragments were employed to transform *B. subtilis* 168 cells using a standard transformation procedure (6), with selection for chloramphenicol or spectinomycin resistance, to replace each DnaA-Box cluster sequence with an antibiotic-resistance cassette via double cross-over recombination. Next, to eliminate the cassette, the pCHE11FLP plasmid was introduced into transformants using the standard transformation procedure with kanamycin-resistance selection; cells harboring the plasmid were selected; and recombination between the two FRT sites at the 5' and 3' ends of the cassette, mediated by FLP recombinase, was induced upon incubation on LB plates containing 5 μg $mL^{-1}$ kanamycin at 30°C for 24 hours. Next, several transformants were transferred to plates without antibiotic and cultivated overnight at a temperature non-permissive for replication of pCHE11FLP (37°C), followed by selection of kanamycin-sensitive clones and confirmation of clean deletions in target regions by sequencing.

We thus created six strains harboring deletions of single DnaA-box clusters (DBCs) in an otherwise wild-type background; these were MYA018 (*Δ*DBC[*ΔywcI-vpr*]), MYA019 (*Δ*DBC[*yydA–yycS*]), MYA155 (*Δ*DBC[*gcp–ydiF*]), MYA156 (*Δ*DBC[*yqeG–sda*]), MYA157 (*Δ*DBC[*ywlB–ywlC*]), and MYA158 (*Δ*DBC[*jag–thdF*]). To construct a strain harboring simultaneous deletions of the six

DnaA-box clusters (MYA143 [Δ6]), the single deletions were introduced sequentially into the wild-type 168 genome, by replacing each DnaA-box cluster with a drug-resistance cassette followed by cassette removal.

**Transcriptome analysis using an Affymetrix tiling array**

To assess the effects of deletions of DnaA-box clusters on transcription of neighboring genes, we compared the transcriptome profiles of wild-type, Δ*yydA*, Δ5, and Δ6 cells using a custom Affymetrix tiling array that we developed previously (7). RNA extraction, synthesis of complementary DNA, terminal labeling, and hybridization with the tiling array were performed according to the Affymetrix instruction manual. In the present study, the hybridization intensities of cDNA are normalized to a mean of 500, and the average signal intensities of probes in coding sequences were calculated for each gene (Fig. S12 and Table S5 and S6). The array design and the array data of this study have been submitted to the ArrayExpress database (http://www.ebi.ac.uk/microarray-as/ae/) under accession code A-AFFY-161 (array design) and E-MEXP-3069 (transcriptome).

Direct activation of Sda expression and autorepression of DnaA have been well-characterized in *B. subtilis* (8,9). In addition, we previously reported that, among genes adjacent to DBCs, *ywlC* and *yydA* are directly repressed by DnaA during growth in PAB medium (10). The expression levels of genes adjacent to DBCs in Δ6 cells are summarized in Table S6. Although the DBC in the *dnaA* promoter region was not manipulated, the level of expression of the *dnaAN* operon in Δ6 cells was significantly reduced compared to that of wild-type cells. As the expression level of DnaA was

maintained in Δ6 cells (Fig. S5), the reduction in *dnaAN* expression must result from autogenous regulation of DnaA. Deactivation of *sda* was not obvious in Δ6 cells, probably because of low-level *sda* expression under our growth conditions, thus in SMM medium at 30°C. The expression of *ywlC* was not affected in Δ6 cells, suggesting that the DnaA-boxes remaining downstream of the *ywlC* promoter (Fig. S1C) may be important for regulation of *ywlC* expression. Consistent with removal of the promoter (Fig. S1E) (10), transcription of *yydA* was clearly reduced in Δ6 cells. However, *vpr* and *ywcI-sacT* were notably derepressed, and *thdF-gidAB–yyaA* inhibited, in Δ6 cells. DnaA might act as a repressor or activator of these genes, at least under our growth conditions. However, it is also possible that deletion of DBC removed the binding sites for other transcriptional regulators, Indeed, two ComK-binding sites located near DBC[*thdF-jag*] positively regulate transcription of the *thdF* operon (11), and a LexA-binding site within DBC[*ywcL-vpr*] is expected to be involved in repression of transcription of the *vpr* gene (12). Further work is necessary to explore the possible direct involvement of DnaA in the regulation of gene expression in these regions.

Further, and interestingly, transition-state genes repressed by AbrB during the exponential growth phase (the AbrB regulon) (7) were strongly induced in Δ6 and Δ5 cells (Fig. S12 and Table S6). Elucidation of the mechanism inducing the AbrB regulon will be both interesting and important. In addition, the SigD regulon (13) appeared to be downregulated in Δ6 cells, although the data were not well reproducible.

**Quantitative measurement of DnaA-bound DNA by real-time PCR**

Using strains expressing the DnaA protein C-terminally tagged with 12 histidines

(DnaA-His), DnaA-bound DNA fragments were co-precipitated with DnaA-His using chromatin affinity purification (ChAP), as previously described (10,14). Chromosomal DNA was also purified in the same manner from a crude cell lysate after sonication, and used as a normalization standard in quantitative PCR analysis.

To measure the amounts of DNA co-purifying with DnaA, by real-time quantitative PCR, primer sets amplifying the *oriC* (RTrpmH-dnaA.f and RTrpmH-dnaA.r) and *yydA-yycS* regions (RTyydA-yycS.f and RTyydA-yycS.r) were designed using Primer3 software (http://frodo.wi.mit.edu/primer3/input.htm) (Table S3). 5' region of *rapA* gene, where is DnaA-binding negative in previous DnaA ChAP-chip analysis (10) and is proximal to *yydA-yycS* region, was also selected for this analysis to calculate background value (oHO274 and oHO275). Real-time quantitative PCR was achieved using a LightCycler 480 Real-Time PCR System (Roche), according to the protocol of the supplier. After background subtraction, amount of DNA co-purified with DnaA was shown as a relative amount to that of *yydA-yycS* region on the genome.

**Construction of strains (see also Table S1)**

**HO1009 (Δ5):** The deletion of the *yydA–yycS* region in MYA143 (Δ6) was restored to wild-type status using a negative selection marker cassette harboring the *mazF* toxin gene (15), as schematically shown in Fig. S2.

**MU01:** To construct the MU01 strain, in which chromosomal replication was conducted in a DnaA-independent manner, the entire *oriC* sequence and the *dnaA* gene were replaced with the *oriN* (*repN* gene and promoter) sequence of the *B. subtilis* var. *natto*

plasmid pLS32 (16), as schematically illustrated in Fig. S8. Briefly, the chromosomal sequence between *rpmH* (encoding the 50S ribosomal protein L34) and *yaaA* (a gene of unknown function) was replaced by the *oriN* sequence, accompanied by a spectinomycin-resistance cassette as a selection marker. In addition, to ensure expression of *dnaN* and *rpmH*, we placed the *dnaN* gene under the control of the constitutive *rpmGA* promoter (P*rpmGA*), placed in front of the *rpmH* gene. To this end, DNA fragments containing *rnpA* and *rpmH* (F1), the *dnaN* coding sequence (F2), P*rpmGA* (F3), and the *yaaH* gene (F6), were amplified from wild-type 168 chromosomal DNA using the primers indicated in Table S3. The *oriN* sequence and the spectinomycin-resistance cassette were amplified from *B. subtilis* NIS6301 (*spoIIIJ*::pRKl, *ΔoriC*) chromosomal DNA (17) and the pAPNC213 plasmid (18), respectively. The resulting PCR products were ligated in the order F1-F2-F3-F4-F5-F6, using three recombinant PCR steps, and wild-type 168 cells were transformed with the ligated fragment followed by selection for spectinomycin resistance.

Although flow cytometry analysis showed merger of the 2N and 4N peaks, suggesting that chromosomal replication was asynchronous in MU01 cells, the growth rate and cell morphology of such cells grown in SMM medium were similar to those of wild-type cells (data not shown).

**MU02:** We created plasmid pXTt-MCS to integrate genes of interest, together with a xylose-inducible P*xyl* promoter, into the *amyE* locus of the *B. subtilis* chromosome, utilizing Gateway technology, as schematically illustrated in Fig. S9. To this end, a strong transcriptional terminator of *E. coli rrnB* was amplified from the pMUTinNC plasmid (18) using Ter-F and TerR-*Sma*I primers, and joined to a *tet* cassette, amplified

by recombinant PCR from plasmid pBEST307, using tet2F and tetT-TerF primers. Next, the resultant fragment was cloned between two *Eco*RV sites in the pX plasmid (19), harboring *amyE*-up and *amyE*-down sequences, together with the P*xyl* promoter and the *xylR* repressor gene, creating plasmid pXTt. Next, pXTt was converted to a destination vector by insertion of a Gateway cassette amplified from plasmid pUC19-yfpGWsp using yfpGWSp-F(XbaI) and yfpGWSp-R(BglII) primers, to create plasmid pXTtGW. The pUC19-yfpGWsp plasmid was constructed by substituting the *cat* gene lying between two *Bam*HI sites in the pUC19-yfpGW plasmid (4) with the *spec* gene amplified from plasmid pAPNC213 (18), using SPCF and specR-ESKSBX primers. The pXTtGW plasmid was further converted to the pXTt-MCS plasmid by recombination with pENTR-MCS, a Gateway entry clone harboring the multiple cloning site (MCS) sequence of pUC19, created by recombination between the pDONR201 vector and the MCS sequence amplified from the pUC19 plasmid using pUCMCS-F-adapter and pUCMCS-R-adapter primers.

Originally, we planned to clone the *dnaA* gene using pXTtGW, employing Gateway technology, or to insert the gene into the MCS of pXTt-MCS, and to integrate the resulting construct into the *B. subtilis* chromosome. However, we found that DnaA expression levels in strains constructed using this procedure were rather low, because of the presence of a ribosome binding sequence (RBS) between P*xyl* and the MCS (data not shown). Thus, to remove the RBS, the *dnaA* gene was directly fused to P*xyl* by recombinant PCR, and next integrated into the chromosome of the 168M strain, as schematically illustrated in Fig. S10. Two fragments, harboring *xylR*-P*xyl* and *amyE*-back sequences, were amplified from pXTt-MCS using the primer sets Pxyl-F/Pxyl-SD-R2 and amyE-backF/amyE-backR, respectively. In addition, an

erythromycin-resistance cassette was amplified from pMUTinNC using erm-F2 and erm-R primers, and the *dnaA* gene was amplified from wild-type 168 chromosomal DNA employing dnaAF-SDR2 and dnaAr-ErmF2 primers. The fragments were ligated in the order [*xylR*-P*xyl*]-[*dnaA*]-[*erm*]-[a*myE*-back] by recombinant PCR, and the construct introduced into the 168M chromosome via double-crossover recombination, to create strain MU02.

**HO1001 (*ΔyydA::tet*):** Sequences upstream and downstream of the *yydA* gene were amplified from the wild-type 168 chromosome using the primer sets yydA-yycS.f5/yydA-yycS.r5 and yydA-yycS.f6/yydA-yycS.r2, respectively, and ligated to a tetracycline-resistance cassette amplified from the pBEST307 plasmid (20), using rPCR-tetF and rPCR-tetR primers, by recombinant PCR. Wild-type 168 cells were transformed with the ligated fragment, to create the HO1001 strain.

**HO1010 (*ΔyydA::tet, orf1[ochre]*) and HO1011 (*ΔyydA::tet, orf2[ochre]*)**: To introduce an ochre mutation into *orf1* identified in the intergenic region between *yydA* and *yycS* (Fig. S13B), the 3' portion of *orf1*, together with the *tet* gene, and the 5' region, were amplified from the HO1001 (*ΔyydA::tet*) chromosome using the primer sets yydA-yycS.f5/och1-r and och1-f/yydA-yycS.r4, respectively. We introduced base changes into the och1-r and och1-f primers to introduce an ochre mutation into *orf1*. The two PCR products were ligated by recombinant PCR, and used to transform wild-type 168 cells, to create the HO1010 strain. HO1011 was made by the same procedure using the primer sets yydA-yycS.f5/och2-r and och2-f/yydA-yycS.r4.

**HO1072 and HO1073 (*Δspo0J::tet*):** Sequences upstream and downstream of *spo0J* were amplified from the wild-type 168 chromosome using the primer sets spo0J.f1/spo0J.r1 and spo0J.f2/spo0J.r2, respectively, and ligated with the *tet* cassette from pBEST307 by recombinant PCR. Wild-type 168 and MYA143 (Δ6) cells were transformed with the PCR product, to create the HO1072 and HO1073 strains, respectively.

**HO1243, HO1244, HO1245, and HO1246**: To insert DBC[*yqeG-sda*], DBC[*ywlC-ywlB*], DBC[*ywcI-vpr*], DBC[*thdF-jag*], or DBC[*gcp-ydiF*] at intergenic region between *yydA-yycS*, these fragments were amplified from the wild-type 168 chromosome using the primer sets oHO259/oHO260, oHO261/oHO262, oHO263/oHO264, oHO265/oHO266, and oHO292/oHO258, respectively. The 5' region of [*yydA-yycS*], together with the *tet* gene, and the 3' region, were amplified from the HO1001 (*ΔyydA::tet*) chromosome using the primer sets yydA-yycS.f5/rPCR-tetF and oHO256/pMB0048, respectively and ligated with respective DBC fragments by recombinant PCR. The resultant PCR fragments were used to transform MYA143 cells, to create the HO1243, HO1244, HO1245, and HO1246 strains, respectively.

**HO1019, HO1020, HO1021, HO1022, and HO1023**: To insert the DBC[*yydA-yycS*] fragment into various sites of the MYA143 (Δ6) chromosome, the *yydA-yycS* fragment was amplified together with the tetracycline-resistance cassette (*tet*) from the HO1001 (*ΔyydA::tet*) chromosome using the yydA-yycS.r2 and yydA.f1 primers. Sequences upstream and downstream of the target sites of the *yydA-yycS* insertion were amplified from the wild-type 168 chromosome using the primer sets indicated in Table S3, and

ligated with the *tet* cassette from pBEST307 by PCR, followed by transformation of MYA143 cells. In the present study, we replaced the *yabT* (7°), *yhaR* (90°), *ypqA* (200°), *yteA* (270°), and *yxbC* (353°) genes (the expression of which was not detected during exponential phase, using an array method [13]) with the DBC[*yydA-yycS*] sequence to create strains HO1019, HO1020, HO1021, HO1022, and HO1023, respectively.

**HO1038, and HO1039**: For integration of the DBC[*yydA-yycS*] fragment into *cgeD*(180°) and *yonN*(190°) sites of the MYA143 (Δ6) chromosome, different antibiotic markers, *erm* and *cat* cassettes, were amplified from pMUTinNC and pDLT3, respectively. DBC[*yydA-yycS*] fragment was amplified from the wild-type 168 chromosome using the primer set oHO253/oHO254. Sequences upstream and downstream of the target sites of the *yydA-yycS* insertion were amplified from the wild-type 168 chromosome using the primer sets indicated in Table S3, and ligated with the antibiotic cassettes and DBC[*yydA-yycS*] fragment, followed by transformation of MYA143 cells.

**Strains harboring the *tetO* array and the *tetR*-mCherry gene**: To visualize the locations of chromosomal *oriC* regions within cells, chromosomal DNA of the JWV086 strain (8) harboring the *tetO* array at the *hutM* locus (353°) and the *tetR*-mCherry gene at the *amyE* locus (353°), was used to transform strains to be examined, employing selection for resistance to spectinomycin and kanamycin .

**HO1029 (Δ5 *dnaA-12his*) and HO1128 (Δ6 *dnaA-12his*):** To insert a sequence encoding 12 histidines at the 3' end of the authentic *dnaA* gene, pMUTinAhisN was

introduced into the MYA143 (Δ6) and HO1009 (Δ5) chromosomes, followed by removal of plasmid sequences, as previously described (10).

**HO1012, HO1016, and HO1192 harboring pBOX-DBC[*yydA-yycS*]:** To insert the DBC sequence between *yydA* and *yycS* into a multicopy plasmid, DBC[*yydA-yycS*] was amplified from the wild-type 168 chromosome using yydA-yycS.f1 and yydA-yycS.r1 primers, digested with *Bbe*I and *Eco*RI, and inserted into the pO2HC plasmid (4). The resulting pBOX-DBC[yydA-yycS] plasmid was introduced into the wild-type, MYA143 (Δ6), and HO1128 (Δ6 *dnaA-12his*) strains, to create the HO1012, HO1016, and HO1192 strains, respectively.

**References**


1. Cherepanov, P.P. and Wackernagel, W. (1995) Gene disruption in *Escherichia coli*: TcR and KmR cassettes with the option of Flp-catalyzed excision of the antibiotic-resistance determinant. *Gene*, **158**, 9-14.

2. Datsenko, K.A. and Wanner, B.L. (2000) One-step inactivation of chromosomal genes in *Escherichia coli* K-12 using PCR products. *Proc Natl Acad Sci U S A*, **97**, 6640-6645.

3. Fukuchi, K., Kasahara, Y., Asai, K., Kobayashi, K., Moriya, S. and Ogasawara, N. (2000) The essential two-component regulatory system encoded by *yycF* and *yycG* modulates expression of the *ftsAZ* operon in *Bacillus subtilis*. *Microbiology*, **146 ( Pt 7)**, 1573-1583.

4. Ishikawa, S., Kawai, Y., Hiramatsu, K., Kuwano, M. and Ogasawara, N. (2006) A new FtsZ-interacting protein, YlmF, complements the activity of FtsA during progression of cell division in *Bacillus subtilis*. *Mol Microbiol*, **60**, 1364-1380.

5. Ochi, K., Kim, J.Y., Tanaka, Y., Wang, G., Masuda, K., Nanamiya, H., Okamoto, S., Tokuyama, S., Adachi, Y. and Kawamura, F. (2009) Inactivation of KsgA, a 16S rRNA methyltransferase, causes vigorous emergence of mutants with high-level kasugamycin resistance. *Antimicrob Agents Chemother*, **53**, 193-201.

6. Anagnostopoulos, C. and Spizizen, J. (1961) Requirements for transformation in *Bacillus subtilis*. *Journal of Bacteriology*, **81**, 741.

7. Chumsakul, O., Takahashi, H., Oshima, T., Hishimoto, T., Kanaya, S., Ogasawara, N. and Ishikawa, S. (2011) Genome-wide binding profiles of the *Bacillus subtilis* transition state regulator AbrB and its homolog Abh reveals their interactive role in transcriptional regulation. *Nucleic Acids Res*, **39**, 414-428.

8. Veening, J.W., Murray, H. and Errington, J. (2009) A mechanism for cell cycle regulation of sporulation initiation in *Bacillus subtilis*. *Genes Dev*, **23**, 1959-1970.

9. Burkholder, W.F., Kurtser, I. and Grossman, A.D. (2001) Replication initiation proteins regulate a developmental checkpoint in *Bacillus subtilis*. *Cell*, **104**, 269-279.

10. Ishikawa, S., Ogura, Y., Yoshimura, M., Okumura, H., Cho, E., Kawai, Y., Kurokawa, K., Oshima, T. and Ogasawara, N. (2007) Distribution of stable DnaA-binding sites on the *Bacillus subtilis* genome detected using a modified ChIP-chip method. *DNA Res*, **14**, 155-168.

11. Ogura, M., Yamaguchi, H., Kobayashi, K., Ogasawara, N., Fujita, Y. and Tanaka,

T. (2002) Whole-genome analysis of genes regulated by the *Bacillus subtilis* competence transcription factor ComK. *J Bacteriol*, **184**, 2344-2351.

12. Au, N., Kuester-Schoeck, E., Mandava, V., Bothwell, L.E., Canny, S.P., Chachu, K., Colavito, S.A., Fuller, S.N., Groban, E.S., Hensley, L.A. *et al.* (2005) Genetic composition of the *Bacillus subtilis* SOS system. *J Bacteriol*, **187**, 7655-7666.

13. Serizawa, M., Yamamoto, H., Yamaguchi, H., Fujita, Y., Kobayashi, K., Ogasawara, N. and Sekiguchi, J. (2004) Systematic analysis of SigD-regulated genes in *Bacillus subtilis* by DNA microarray and Northern blotting analyses. *Gene*, **329**, 125-136.

14. Cho, E., Ogasawara, N. and Ishikawa, S. (2008) The functional analysis of YabA, which interacts with DnaA and regulates initiation of chromosome replication in *Bacillus subtilis*. *Genes & genetic systems*, **83**, 111-125.

15. Morimoto, T., Ara, K., Ozaki, K. and Ogasawara, N. (2009) A new simple method to introduce marker-free deletions in the *Bacillus subtilis* genome. *Genes Genet Syst*, **84**, 315-318.

16. Tanaka, T., Ishida, H. and Maehara, T. (2005) Characterization of the replication region of plasmid pLS32 from the Natto strain of *Bacillus subtilis*. *J Bacteriol*,

**187**, 4315-4326.

17. Moriya, S., Hassan, A.K., Kadoya, R. and Ogasawara, N. (1997) Mechanism of anucleate cell production in the oriC-deleted mutants of *Bacillus subtilis*. *DNA Res*, **4**, 115-126.

18. Morimoto, T., Loh, P.C., Hirai, T., Asai, K., Kobayashi, K., Moriya, S. and Ogasawara, N. (2002) Six GTP-binding proteins of the Era/Obg family are essential for cell growth in *Bacillus subtilis*. *Microbiology*, **148**, 3539-3552.

19. Kim, L., Mogk, A. and Schumann, W. (1996) A xylose-inducible *Bacillus subtilis* integration vector and its application. *Gene*, **181**, 71-76.

20. Itaya, M. (1992) Construction of a novel tetracycline resistance gene cassette useful as a marker on the *Bacillus subtilis* chromosome. *Bioscience, biotechnology, and biochemistry*, **56**, 685-686.

21. Kunst, F., Ogasawara, N., Moszer, I., Albertini, A., Alloni, G., Azevedo, V., Bertero, M., Bessieres, P., Bolotin, A. and Borchert, S. (1997) The complete genome sequence of the gram-positive bacterium *Bacillus subtilis*. *Nature*, **390**.

22. Ishikawa, S., Hara, Y., Ohnishi, R. and Sekiguchi, J. (1998) Regulation of a new cell wall hydrolase gene, *cwlF*, which affects cell separation in *Bacillus subtilis*. *J Bacteriol*, **180**, 2549-2555.

**Supplementary Figure legends**

**Figure S1. Schematic representation of the arrangements of genes, DnaA-boxes, and promoter sequences around the six DBCs deleted in the Δ6 strain.**

The structures of the intergenic regions of *gcp-ydiF* (A), *yqeG-sda* (B), *ywlC-ywlB* (C), *ywcI-vpr* (D), *yydA-yycS* (E), and *thdF-jag* (F) are schematically presented, together with neighboring genes. The locations and directions of protein-encoding genes and DnaA-boxes are shown using thick open and closed arrows, respectively. Thin arrows indicate the positions and directions of possible promoter sequences. Sequences deleted in the Δ6 strain are indicated below the panels, and genome coordinates from the original report (21) are indicated below and above each panel.

**Figure S2. Construction of the Δ5 strain.**

" See text and inserted explanation in this figure".

**Figure 3. Flow cytometry profiles of double DBC mutants and Δ6-DBC mutants.**

Flow cytometry profiles of double DBC deletion mutants containing ΔDBC[*yydA-yycS*] (B-F) and Δ6 mutants with single insertion of another DBC at deleted region of *yydA-yycS* (353°) (H-L). Profiles of the (A) MYA019 (ΔDBC[*yydA-yycS*]), (G) MYA143 (Δ6), and (J) HO1023 (Δ6 353°::DBC[*yydA-yycS*]) strains in Figure 1 are also shown for comparison. (B) HO1231 (ΔDBC[*yydA-yycS*] ΔDBC[*yqeG-sda*]), (C) HO1232 (ΔDBC[*yydA-yycS*] ΔDBC[*ywlC-ywlB*]), (D) HO1233 (ΔDBC[*yydA-yycS*]

ΔDBC[*ywcI-vpr*]), (E) HO1234 (ΔDBC[*yydA-yycS*] ΔDBC[*thdF-jag*]), (F) HO1230 (ΔDBC[*yydA-yycS*] ΔDBC[*gcp-ydiF*]), (H) HO1243 (Δ6 ΔDBC[*yydA-yycS*]::DBC[*yqeG-sda*]), (I) HO1244 (Δ6 ΔDBC[*yydA-yycS*]::DBC[*ywlC-ywlB*), (K) HO1245 (Δ6 ΔDBC[*yydA-yycS*]::DBC[*ywcI-vpr*]), (L) HO1246 (Δ6 ΔDBC[*yydA-yycS*]::DBC[*thdF-jag*]), and (M) HO1247 (Δ6 ΔDBC[*yydA-yycS*]::DBC[*gcp-ydiF*]).

**Figure S4. Effect of introduction of the pBOX-DBC[*yydA-yycSI*] plasmid into Δ6 cells.**

(A) Flow cytometry profiles of MYA143 (Δ6), HO1015 (Δ6 pO2HC), and HO1016 (Δ6, pBOX-DBC[*yydA-yycS*]) cells, growing in SMM medium at 30°C. (B) The levels of DBC[*yydA-yycS*] fragments bound to DnaA in HO1029 (Δ5 *dnaA-12his*) and HO1192 (Δ6 *dnaA-12his* pBOX-DBC[*yydA-yycS*]) cells. The two strains were grown in LB medium at 37°C to mid-exponential phase, and relative amount of DBC[*yydA-yycS*] fragments bound to DnaA was estimated by ChAP-qPCR, as described in Supplementary materials.

**Figure S5. Cell length distributions of various mutants.**

The lengths of 500~1,000 cells were measured using phase-contrast images taken of various mutant cells exponentially growing in SMM medium at 25°C, and histograms of cell length at 0.5 μm intervals are shown. (A) wild-type (168), (B) MYA143 (Δ6), (C) HO1034 (*Δspo0J*), (D) HO1030 (*Δ[soj-spo0J]*), (E) HO1035 (Δ6 *Δspo0J*), (F) HO1225

(Δ6 *Δspo0J sojT88M*), (G) HO1031 (Δ6, *Δ[soj-spo0J]*), (H) HO1009 (Δ5), (I) HO1021 (Δ6 200°::DBC[*yydA-yycS*]), (J) HO1041 (Δ5 *Δspo0J*), and (K) HO1178 (Δ6 *Δspo0J* 200°::DBC[*yydA-yycS*]). The numbers of cells examined (n) and average cell length (Av) are also indicated in each panel.

**Figure S6. Flow cytometry profiles of *Δspo0J* and *Δ(soj-spo0J)* cells.**

Flow cytometry profiles of (A) wild-type (168), (B) HO1034 (*Δspo0J*), and (C) HO1030 (*Δ*[*soj-spo0J*]) cells, growing exponentially in SMM medium at 30°C, are presented.

**Figure S7 Subcellular locations of origin foci in cells harboring single nucleoids.**

(A-D) The origin region was visualized using TetR-mCherry bound to a *tetO* array at the *oriC*-proximal region of the chromosomes of (A) HO1194 (Δ(*soj-spo0J*)), (B) HO1200 (Δ6 Δ(*soj-spo0J*)), (C) HO1177 (Δ5 *Δspo0J*), (D) HO1179 (Δ6 *Δspo0J* 200°::DBC[yydA-yycS]) strains. The bacteria were grown in SMM at 25°C, and MitoTracker Green FM (membrane) and mCherry (*oriC*) images were acquired (shown in inset of Upper panel). (Upper panel) Histograms of cell length at 0.1 μm intervals for cells harboring one, two, three, four, or more than four foci (in a single nucleoid) are shown using blue, gray, green, and red bars, respectively. The x-axes are scaled identically in upper and lower panels and numbers are indicated in lower panel. (Lower panel) *oriC* positioning was statistically analyzed, with plotting of the distance from each focus to the same pole in each cell (on the x-axis) against cell length (on the y-axis). The positions of foci in cells harboring one, two, or more than two foci (in a

single nucleoid) are indicated by blue, gray, and red points, respectively. The distance between the two *oriC* foci in each cell (interfocal distance, IFD) is indicated in the inset as a function of cell length (CL). (E-I) Histograms of cell length and *oriC* positioning of indicated strains at the top in Figure 3 are also shown for comparison.

**Figure S8. Construction of the MU01 (Δ(*oriC-dnaA*)::*repN*) strain, lacking the entire *oriC* sequence and the *dnaA* gene.**

" See text and inserted explanation in this figure".

**Figure S9. Construction of the pXTt-MCS plasmid.**

" See text and inserted explanation in this figure".

**Figure S10. Construction of the MU02 (*amyE*::P*xyl-dnaA*) strain.**

" See text and inserted explanation in this figure".

**Figure S11. The levels of DnaA protein induced by xylose in MU03 cells, and the growth curves of strains harboring *oriN* sequence, in the presence and absence of xylose.**

(A) MU03 cells exponentially growing in SMM with increasing amounts of xylose were harvested, and the levels of DnaA protein in the same amounts of cell lysates were detected by Western blotting using an anti-DnaA antibody, as described previously. Glucose in SMM was substituted to glycerol (0.5%) to fully induce DnaA from the xylose promoter. (B, C) Growth curves of wild-type (168; closed circles), MU03 (Δ(*oriC-dnaA*)::*oriN* P*xyl-dnaA*; closed triangles), HO1201 (Δ(*oriC-dnaA*)::*oriN*

*Δspo0J* P*xyl-dnaA*; closed squares), HO1203 (Δ(*oriC-dnaA*)::*oriN* Δ6 P*xyl-dnaA*; open triangles), and HO1206 (Δ(*oriC-dnaA*)::*oriN* Δ6 *Δspo0J* P*xyl-dnaA*; open squares) in SMM at 37°C in the absence (B) and presence (C) of xylose (0.2%).

**Figure S12. Comparison of the transcriptome profiles of Δ6, Δ5, ΔDBC[*yydA–yycS*], and wild-type cells.**

Log-scale scatter plots of the transcriptional intensities of genes in Δ6 (A and B), Δ5 (C), and ΔDBC[*yydA-yycS*] (D) cells (y-axis), and in wild-type cells (x-axis). The comparison of the transcriptome profiles of wild-type and Δ6 strains was performed twice. (E) The flow cytometry profiles of wild-type (168), MYA143 (Δ6), OC003 (*ΔabrB*) and 168SDC (*ΔsigD*, (13)) cells exponentially growing in SMM at 30°C are shown. Since the *sigD* mutant forms filamentous cells (22), dissociation of 168SDC cell chains into single cells by sonication was not effective and were remained as unseparated cells showing apparent 4 origins.

**Figure S13. Flow cytometry profiles of the *ΔyydA*, *orf1(ochre)*, and *orf2(ochre)* strains.**

(A) The flow cytometry profiles of wild-type (168), HO1001 (*ΔyydA*), HO1010 (*ΔyydA orf1*[*ochre*]) and HO1011 (*ΔyydA orf2*[*ochre*]) cells exponentially growing in SMM medium at 30°C are shown. (B) The nucleotide sequence of the intergenic region between *yydA* and *yycS*. Blue and red open boxes on the sequence indicate 1-bp mismatched and perfectly matched DnaA-boxes, respectively. Two small orfs (*orf1* and *orf2*) are indicated by green open arrows, and the positions of the introduced ochre

mutations are indicated by asterisks. The position of insertion of the "G" in the revised genome sequence (NC_000964.3), although sequencing showed that our strain had no such insertion, is indicated by a red vertical arrow.

**Figure 14. SOS response is induced in Δ6-*Δspo0J* double mutant cells.**

SOS response was monitored by measuring activity of β-galactosidase expressed from the *dinC* promoter at *amyE* locus (*amyE*::P*dinC-bgaB*). Cells of HO1235 (wild-type), HO1236 (Δ6), HO1237 (*Δspo0J*), HO1251 (Δ6 *Δspo0J*) and HO1248 (*purA*::$P_{IPTG}$-*dnaA*) grown to exponential phase in SMM at 25°C were used. In this experiment, HO1248 cells were also grown in the presence of 20μM IPTG to induce the SOS response by overproduction of DnaA.

**Figure S15. The levels of DnaA protein in the strains of the present study.**

Cells exponentially growing in SMM medium at 30°C were harvested, and the levels of DnaA protein in the same amounts of cell lysates were estimated by Western blotting using an anti-DnaA antibody, as described previously. The relative amount of DnaA was quantified by protein standards for each sample from three independent experiments and normalized to wild-type cells.

(A) 168 (wild-type), MYA155 (ΔDBC[*gcp-ydiF*]) cells, MYA156 (ΔDBC[*ΔyqeG–sda*]), MYA157 (ΔDBC[*ywlC-ywlB*]), MYA018 (ΔDBC[*ywcI-vpr*]), MYA019 (ΔDBC[*yydA-yycS*]), MYA158 (ΔDBC[*thdF-jag*]), HO1009 (Δ5), and MYA143 (Δ6).

(B) HO1019 (Δ6 7°::DBC[*yydA-yycS*]), HO1020 (Δ6 90°::DBC[*yydA-yycS*]), HO1021 (Δ6 200°::DBC[*yydA-yycS*]), HO1022 (Δ6 270°::DBC[*yydA-yycS*]), HO1023 (Δ6

353°::DBC[*yydA-yycS*]), (I) HO1242 (Δ6 180°::DBC[*yydA-yycS*] 200°::DBC[*yydA-yycS*]), HO1241 (Δ6 180°::DBC[*yydA-yycS*] 190°::DBC[*yydA-yycS*] 200°::DBC[*yydA-yycS*]), HO1245 (Δ6 ΔDBC[*yydA-yycS*]::DBC[*ywcI-vpr*]), Δ6 harboring pBOX, and Δ6 harboring pO2HC (no DBC[*yydA-yycS*] insert).

Fig. S1

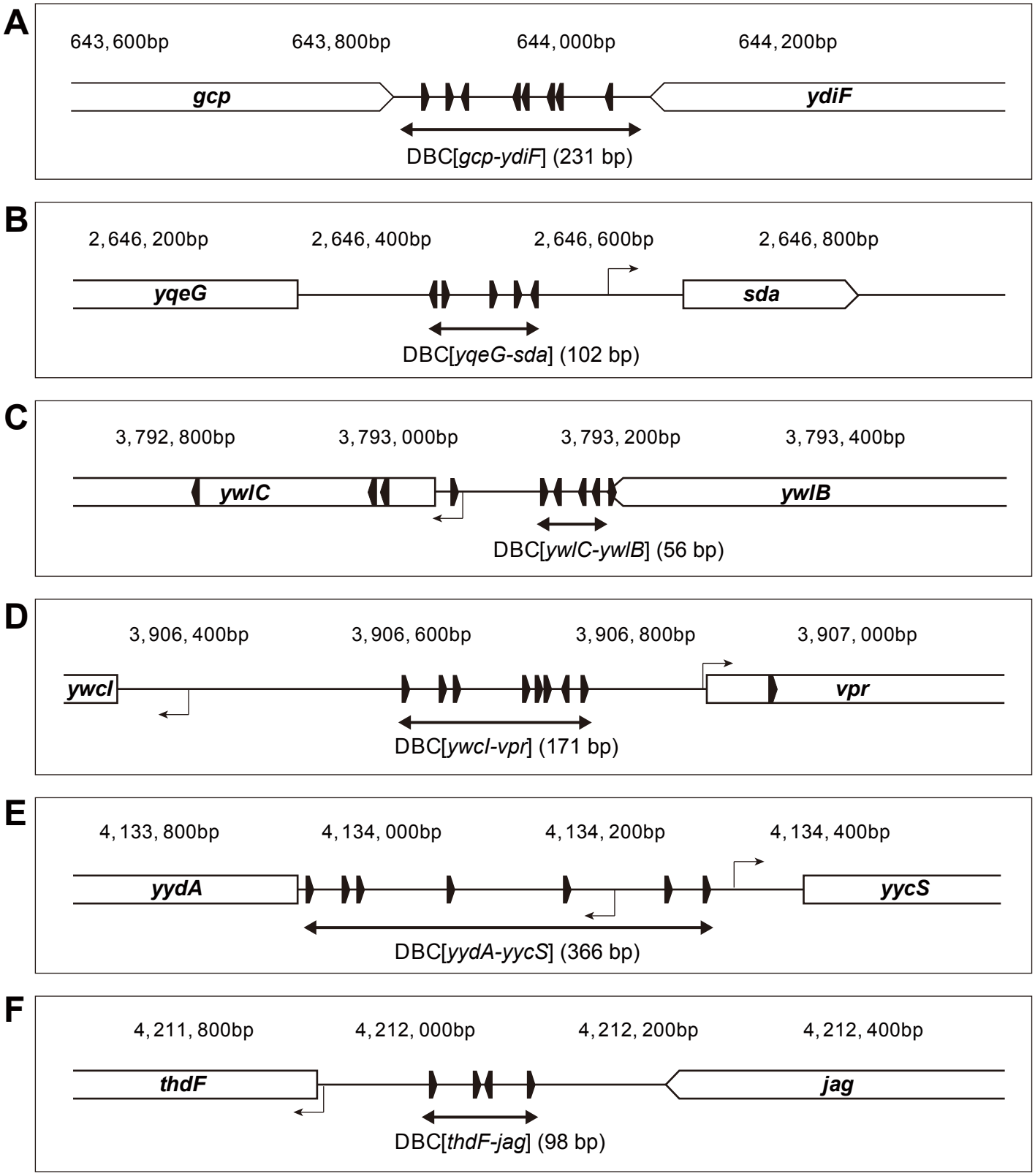
A
643,600bp
643,800bp
644,000bp
644,200bp
gcp
ydiF
DBC[gcp-ydiF] (231 bp)
B
2,646,200bp
2,646,400bp
2,646,600bp
2,646,800bp
yqeG
sda
DBC[yqeG-sda] (102 bp)
C
3,792,800bp
3,793,000bp
3,793,200bp
3,793,400bp
ywlC
ywlB
DBC[ywlC-ywlB] (56 bp)
D
3,906,400bp
3,906,600bp
3,906,800bp
3,907,000bp
ywcI
vpr
DBC[ywcI-vpr] (171 bp)
E
4,133,800bp
4,134,000bp
4,134,200bp
4,134,400bp
yydA
yycS
DBC[yydA-yycS] (366 bp)
F
4,211,800bp
4,212,000bp
4,212,200bp
4,212,400bp
thdF
jag
DBC[thdF-jag] (98 bp)

Fig. S2

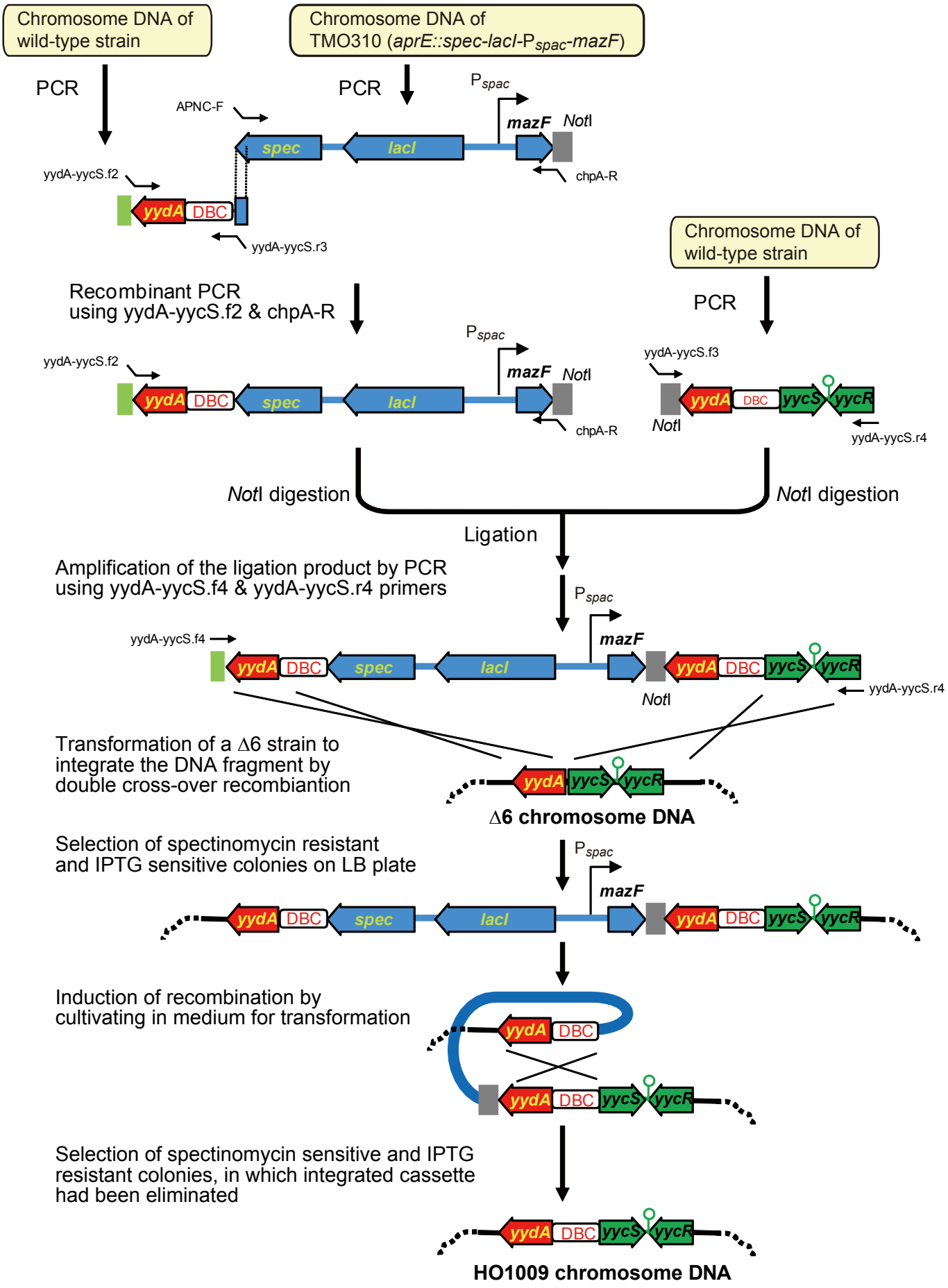
Chromosome DNA of wild-type strain
Chromosome DNA of TMO310 (aprE::spec-lacI-Pspac-mazF)
PCR
PCR
Pspac
APNC-F
mazF
NotI
spec
lacI
chpA-R
yydA-yycS.f2
yydA
DBC
yydA-yycS.r3
Chromosome DNA of wild-type strain
Recombinant PCR using yydA-yycS.f2 & chpA-R
PCR
Pspac
yydA-yycS.f2
mazF
NotI
yydA
DBC
spec
lacI
chpA-R
yydA-yycS.f3
yycS
yycR
NotI
yydA-yycS.r4
NotI digestion
NotI digestion
Ligation
Amplification of the ligation product by PCR using yydA-yycS.f4 & yydA-yycS.r4 primers
Pspac
yydA-yycS.f4
mazF
yydA
DBC
spec
lacI
yycS
yycR
NotI
yydA-yycS.r4
Transformation of a Δ6 strain to integrate the DNA fragment by double cross-over recombiantion
Δ6 chromosome DNA
Selection of spectinomycin resistant and IPTG sensitive colonies on LB plate
Pspac
mazF
Induction of recombination by cultivating in medium for transformation
Selection of spectinomycin sensitive and IPTG resistant colonies, in which integrated cassette had been eliminated
HO1009 chromosome DNA

Fig. S3

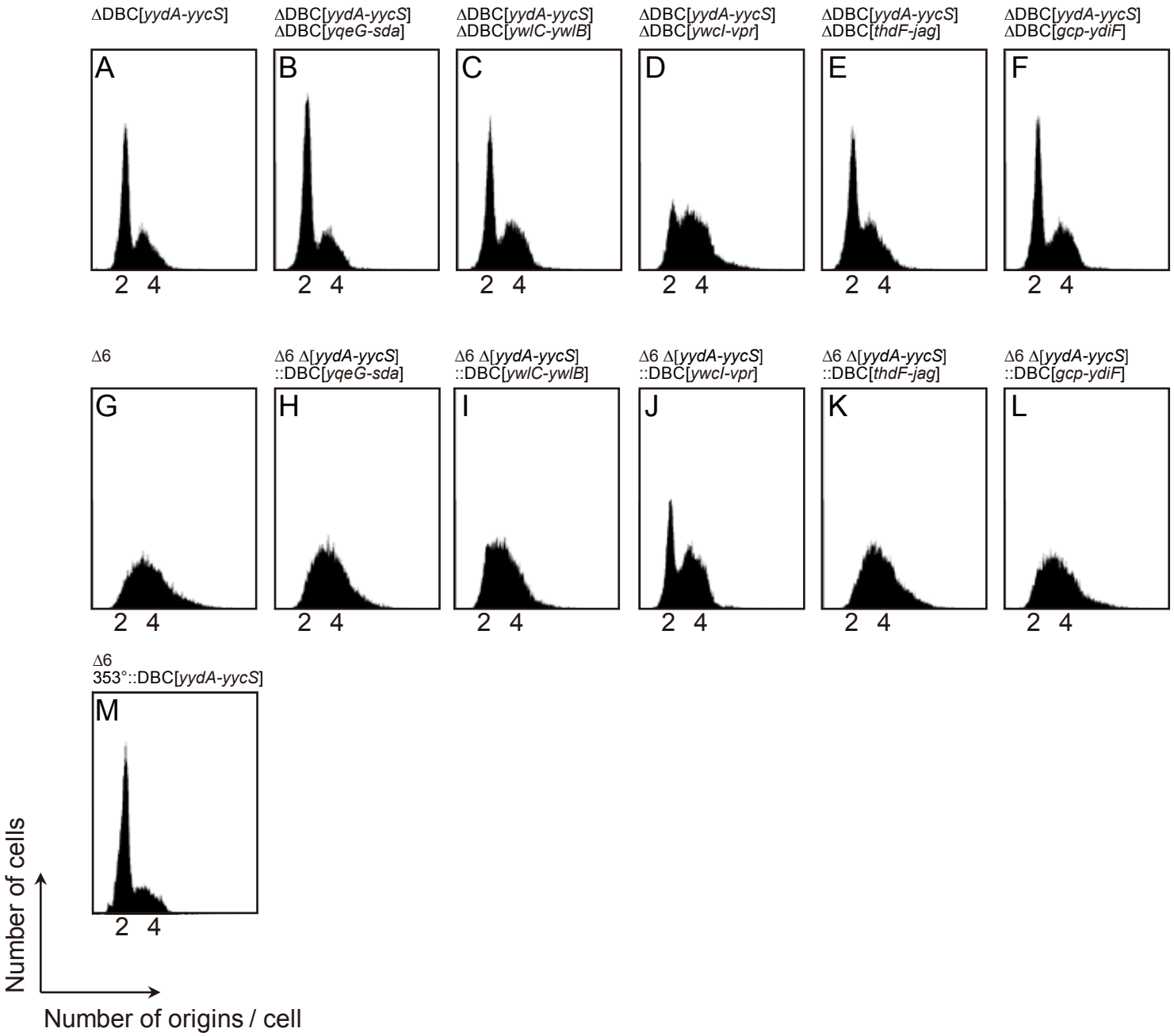
ΔDBC[yydA-yycS]
A
2 4
ΔDBC[yydA-yycS]
ΔDBC[yqeG-sda]
B
2 4
ΔDBC[yydA-yycS]
ΔDBC[ywlC-ywlB]
C
2 4
ΔDBC[yydA-yycS]
ΔDBC[ywcI-vpr]
D
2 4
ΔDBC[yydA-yycS]
ΔDBC[thdF-jag]
E
2 4
ΔDBC[yydA-yycS]
ΔDBC[gcp-ydiF]
F
2 4
Δ6
G
2 4
Δ6 Δ[yydA-yycS]
::DBC[yqeG-sda]
H
2 4
Δ6 Δ[yydA-yycS]
::DBC[ywlC-ywlB]
I
2 4
Δ6 Δ[yydA-yycS]
::DBC[ywcI-vpr]
J
2 4
Δ6 Δ[yydA-yycS]
::DBC[thdF-jag]
K
2 4
Δ6 Δ[yydA-yycS]
::DBC[gcp-ydiF]
L
2 4
Δ6
353°::DBC[yydA-yycS]
M
2 4
Number of cells
Number of origins / cell

Fig. S4

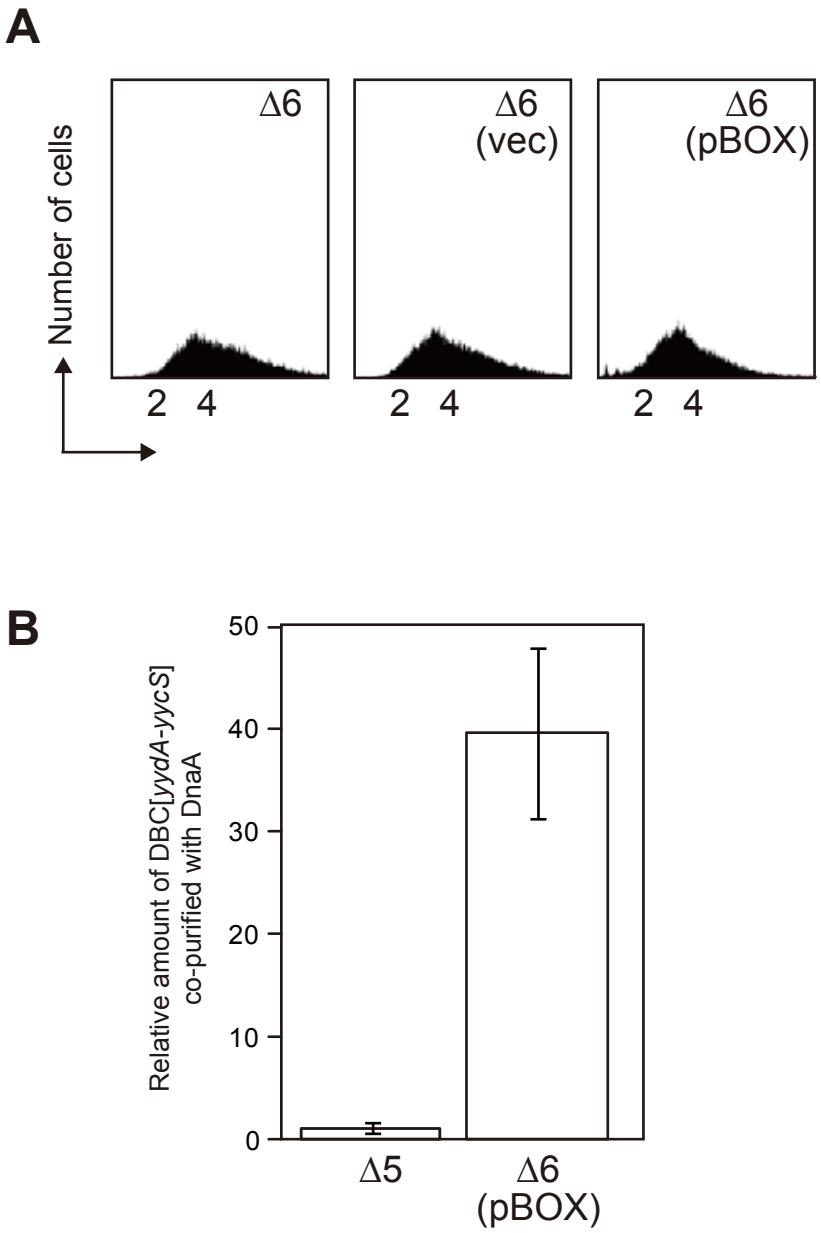
A
Δ6
Δ6
(vec)
Δ6
(pBOX)
Number of cells
2 4
2 4
2 4
B
Relative amount of DBC[yydA-yycS]
co-purified with DnaA
50
40
30
20
10
0
Δ5
Δ6
(pBOX)

Fig. S5

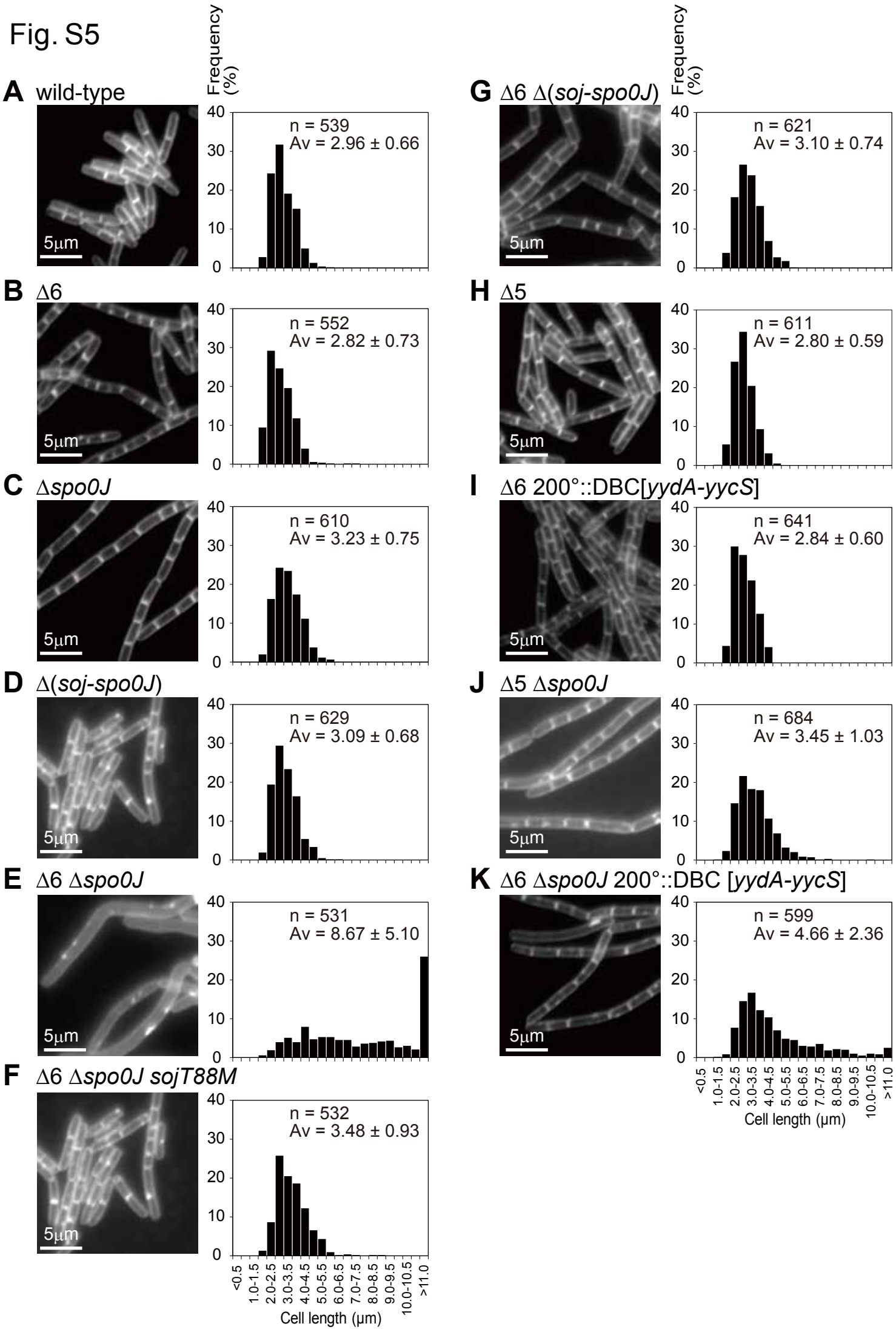
A wild-type
n = 539
Av = 2.96 ± 0.66
B Δ6
n = 552
Av = 2.82 ± 0.73
C Δspo0J
n = 610
Av = 3.23 ± 0.75
D Δ(soj-spo0J)
n = 629
Av = 3.09 ± 0.68
E Δ6 Δspo0J
n = 531
Av = 8.67 ± 5.10
F Δ6 Δspo0J sojT88M
n = 532
Av = 3.48 ± 0.93
G Δ6 Δ(soj-spo0J)
n = 621
Av = 3.10 ± 0.74
H Δ5
n = 611
Av = 2.80 ± 0.59
I Δ6 200°::DBC[yydA-yycS]
n = 641
Av = 2.84 ± 0.60
J Δ5 Δspo0J
n = 684
Av = 3.45 ± 1.03
K Δ6 Δspo0J 200°::DBC [yydA-yycS]
n = 599
Av = 4.66 ± 2.36
Frequency (%)
5μm
<0.5
1.0-1.5
2.0-2.5
3.0-3.5
4.0-4.5
5.0-5.5
6.0-6.5
7.0-7.5
8.0-8.5
9.0-9.5
10.0-10.5
>11.0
Cell length (μm)

Fig. S6

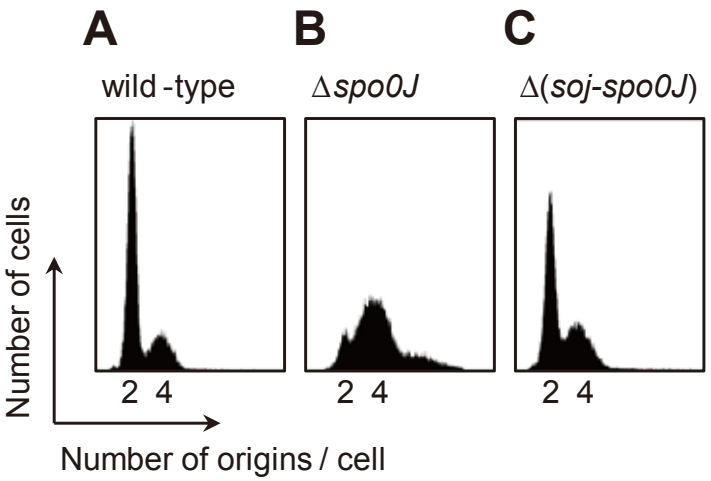
A
B
C
wild -type
Δspo0J
Δ(soj-spo0J)
Number of cells
2 4
2 4
2 4
Number of origins / cell

Fig. S7

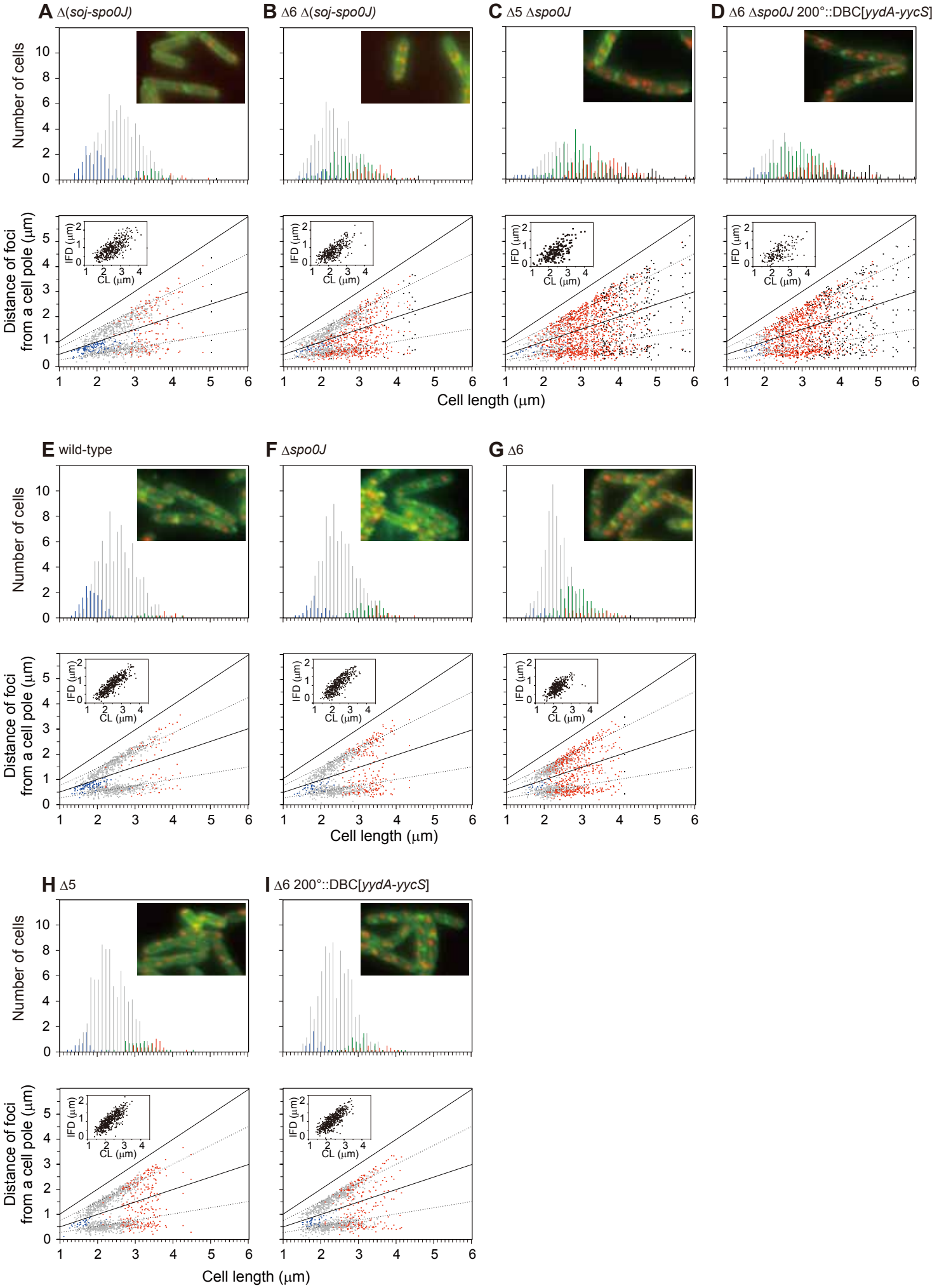
A Δ(soj-spo0J)
B Δ6 Δ(soj-spo0J)
C Δ5 Δspo0J
D Δ6 Δspo0J 200°::DBC[yydA-yycS]
E wild-type
F Δspo0J
G Δ6
H Δ5
I Δ6 200°::DBC[yydA-yycS]
Number of cells
Distance of foci from a cell pole (μm)
IFD (μm)
CL (μm)
Cell length (μm)

Fig. S8

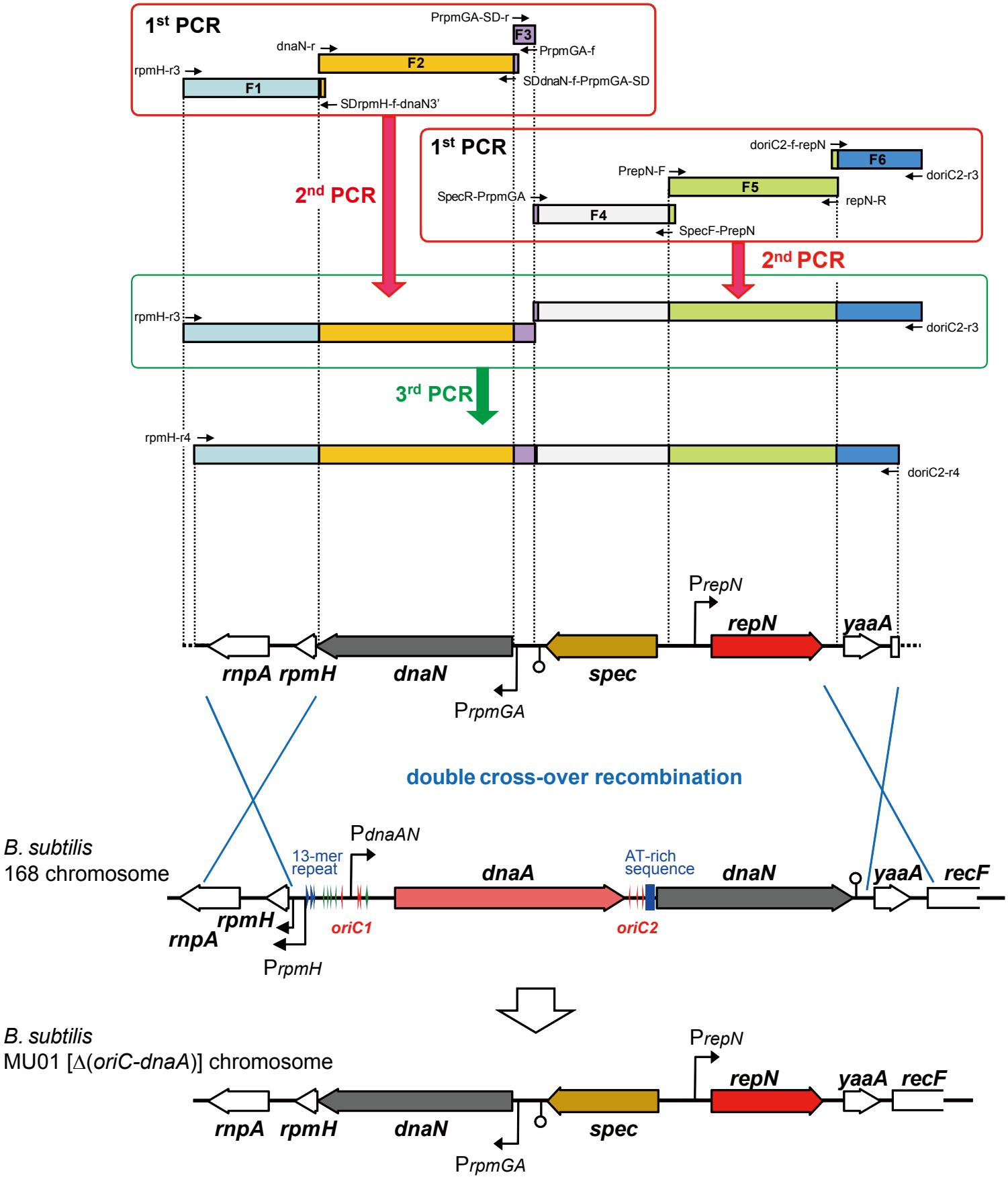
1st PCR
PrpmGA-SD-r
F3
dnaN-r
PrpmGA-f
rpmH-r3
F2
SDdnaN-f-PrpmGA-SD
F1
SDrpmH-f-dnaN3'
1st PCR
doriC2-f-repN
F6
PrepN-F
doriC2-r3
F5
SpecR-PrpmGA
repN-R
F4
SpecF-PrepN
2nd PCR
2nd PCR
rpmH-r3
doriC2-r3
3rd PCR
rpmH-r4
doriC2-r4
PrepN
repN
yaaA
rnpA
rpmH
dnaN
spec
PrpmGA
double cross-over recombination
B. subtilis
168 chromosome
PdnaAN
13-mer repeat
dnaA
AT-rich sequence
dnaN
yaaA
recF
rpmH
rnpA
oriC1
oriC2
PrpmH
B. subtilis
MU01 [Δ(oriC-dnaA)] chromosome
PrepN
repN
yaaA
recF
rnpA
rpmH
dnaN
spec
PrpmGA

Fig. S9

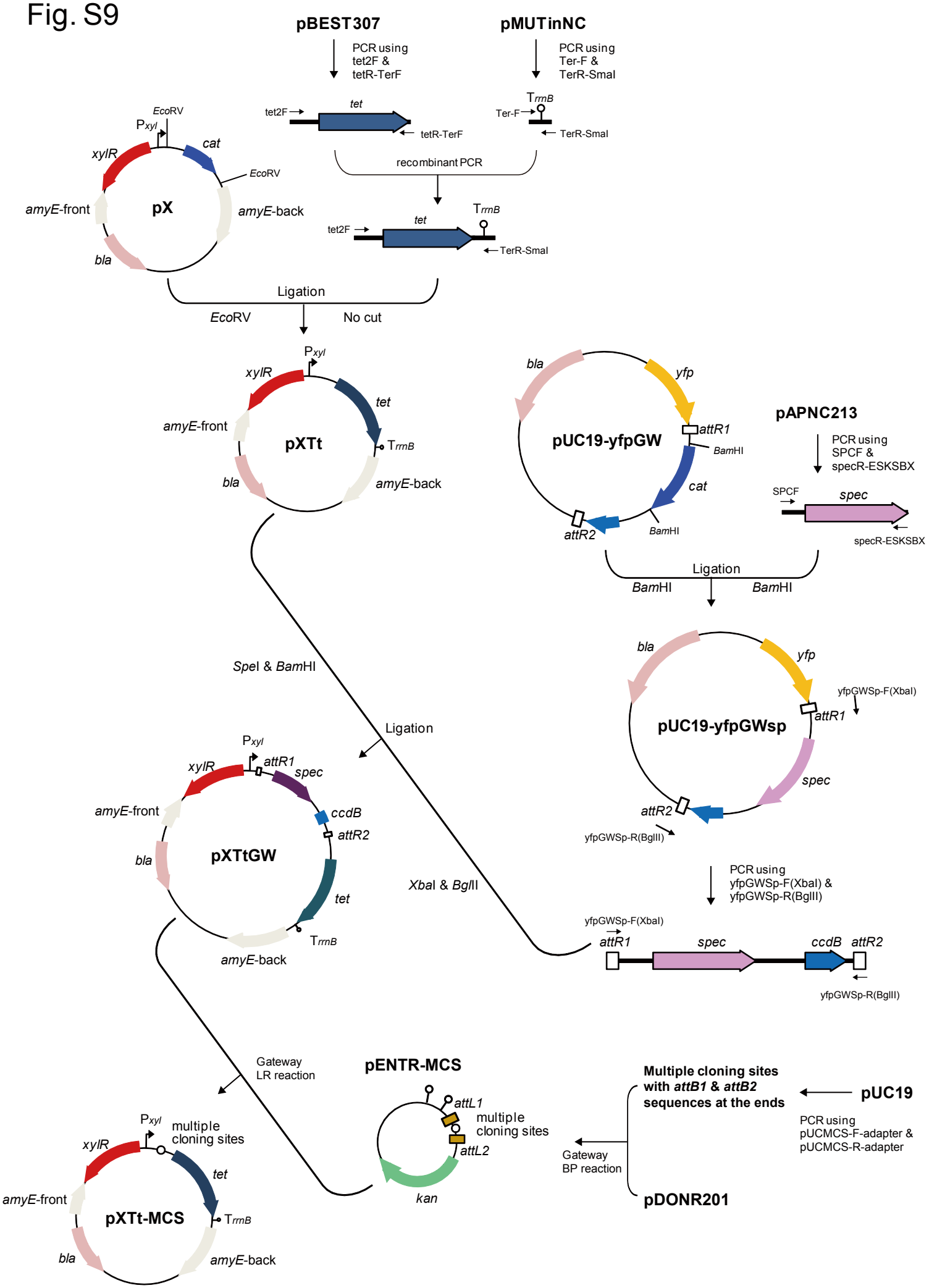
pBEST307
PCR using
tet2F &
tetR-TerF
pMUTinNC
PCR using
Ter-F &
TerR-SmaI
EcoRV
Pxyl
xylR
cat
EcoRV
amyE-front
pX
amyE-back
bla
tet2F
tet
tetR-TerF
TrrnB
Ter-F
TerR-SmaI
recombinant PCR
Ligation
EcoRV
No cut
pXTt
pUC19-yfpGW
yfp
attR1
BamHI
cat
attR2
pAPNC213
PCR using
SPCF &
specR-ESKSBX
SPCF
spec
specR-ESKSBX
Ligation
BamHI
SpeI & BamHI
pUC19-yfpGWsp
yfpGWSp-F(XbaI)
yfpGWSp-R(BglII)
Ligation
pXTtGW
ccdB
XbaI & BglII
PCR using
yfpGWSp-F(XbaI) &
yfpGWSp-R(BglII)
Gateway
LR reaction
pENTR-MCS
attL1
multiple
cloning sites
attL2
kan
pXTt-MCS
Multiple cloning sites
with attB1 & attB2
sequences at the ends
pUC19
PCR using
pUCMCS-F-adapter &
pUCMCS-R-adapter
Gateway
BP reaction
pDONR201

Fig. S10

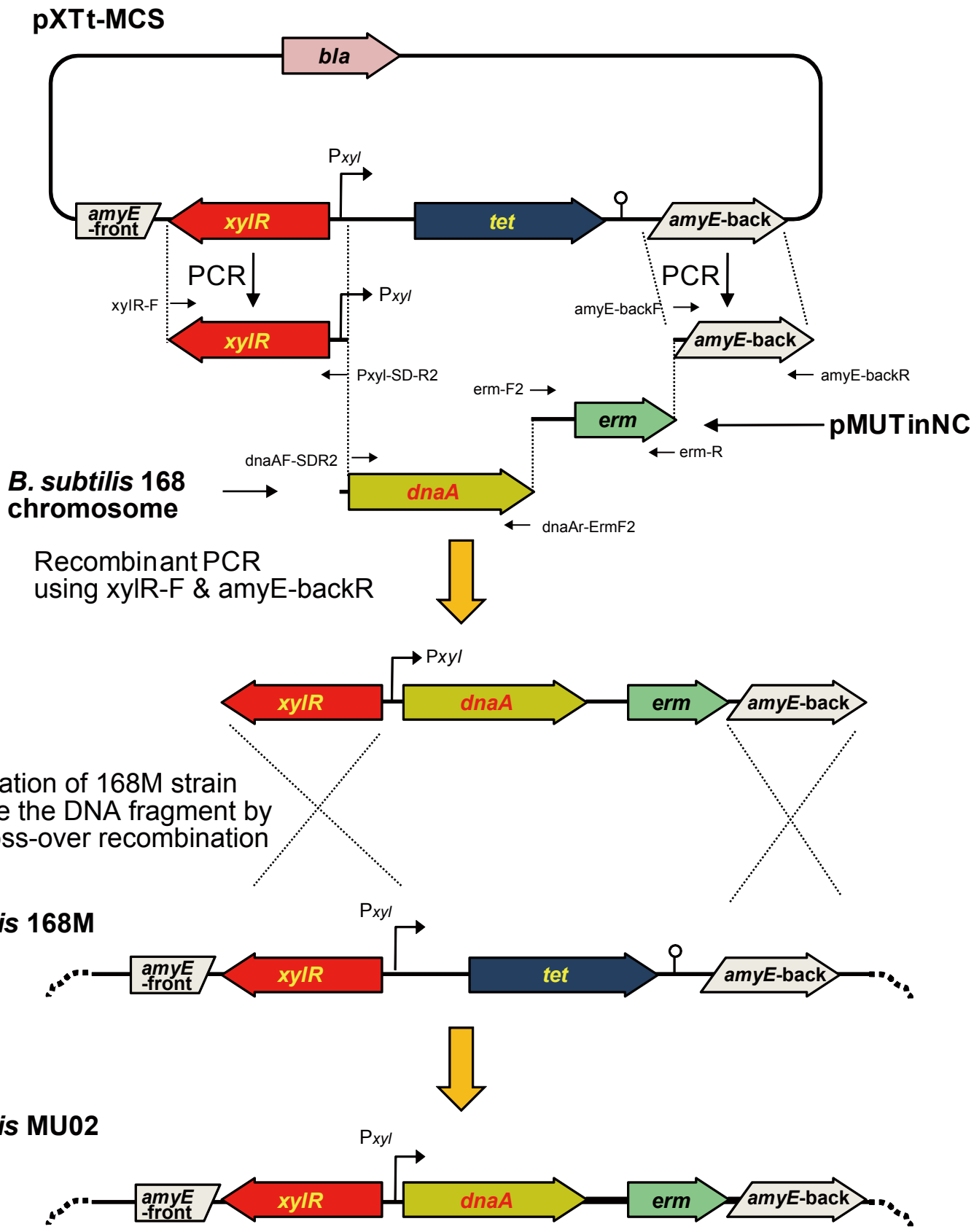
pXTt-MCS
bla
Pxyl
amyE -front
xylR
tet
amyE-back
PCR
PCR
xylR-F
amyE-backF
Pxyl
xylR
amyE-back
Pxyl-SD-R2
amyE-backR
erm-F2
erm
pMUTinNC
erm-R
dnaAF-SDR2
B. subtilis 168 chromosome
dnaA
dnaAr-ErmF2
Recombinant PCR using xylR-F & amyE-backR
Pxyl
xylR
dnaA
erm
amyE-back
Transformation of 168M strain to integrate the DNA fragment by double cross-over recombination
B. subtilis 168M
Pxyl
amyE -front
xylR
tet
amyE-back
B. subtilis MU02
Pxyl
amyE -front
xylR
dnaA
erm
amyE-back

Fig. S11

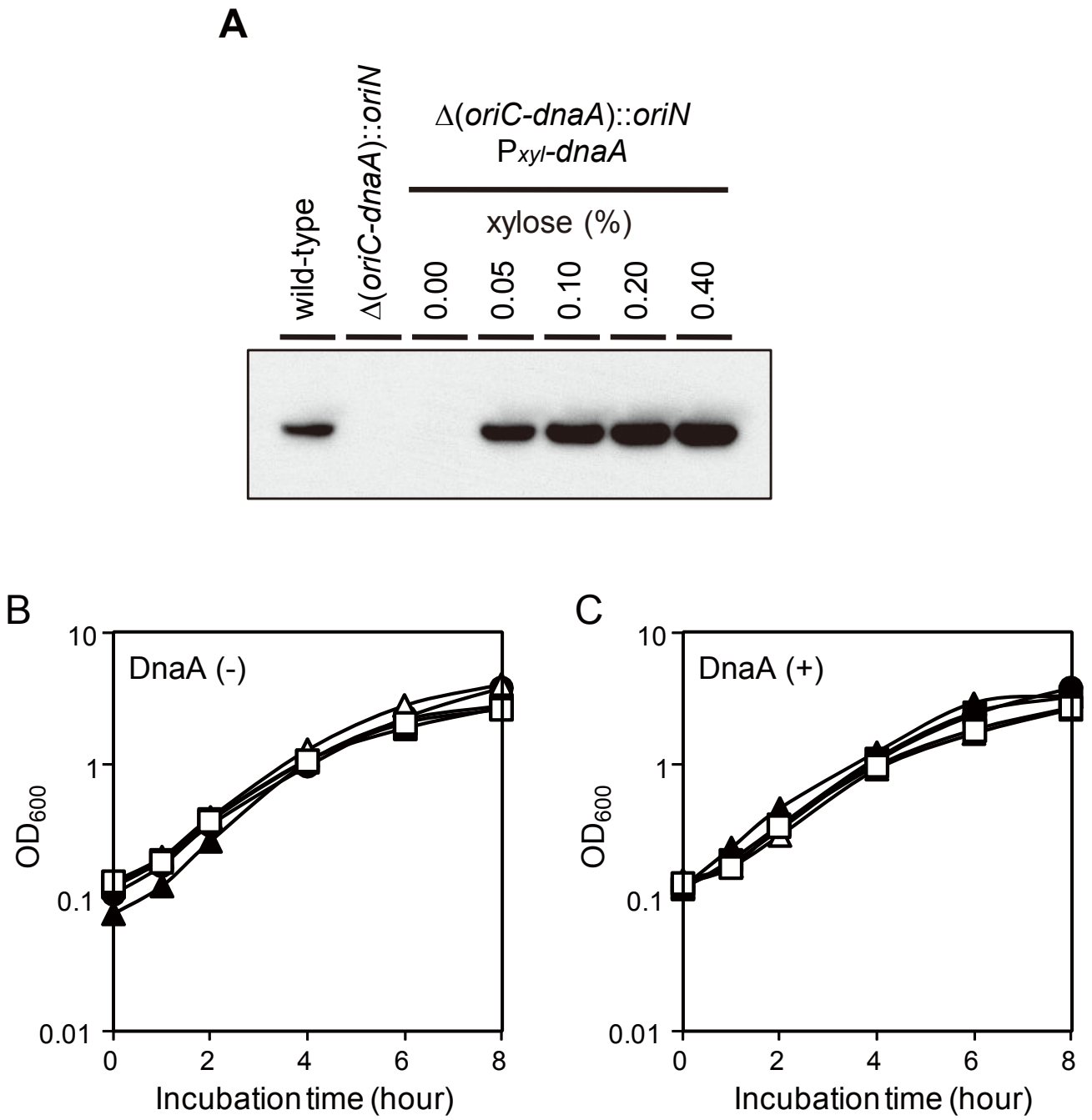
A
wild-type
Δ(oriC-dnaA)::oriN
Δ(oriC-dnaA)::oriN
Pxyl-dnaA
xylose (%)
0.00
0.05
0.10
0.20
0.40
B
DnaA (-)
C
DnaA (+)
OD600
10
1
0.1
0.01
0
2
4
6
8
Incubation time (hour)
● wild-type
▲ Δ(oriC-dnaA)::oriN Pxyl-dnaA
■ Δ(oriC-dnaA)::oriN Δspo0J Pxyl-dnaA
△ Δ(oriC-dnaA)::oriN Δ6 Pxyl-dnaA
□ Δ(oriC-dnaA)::oriN Δ6 Δspo0J Pxyl-dnaA

Fig. S12

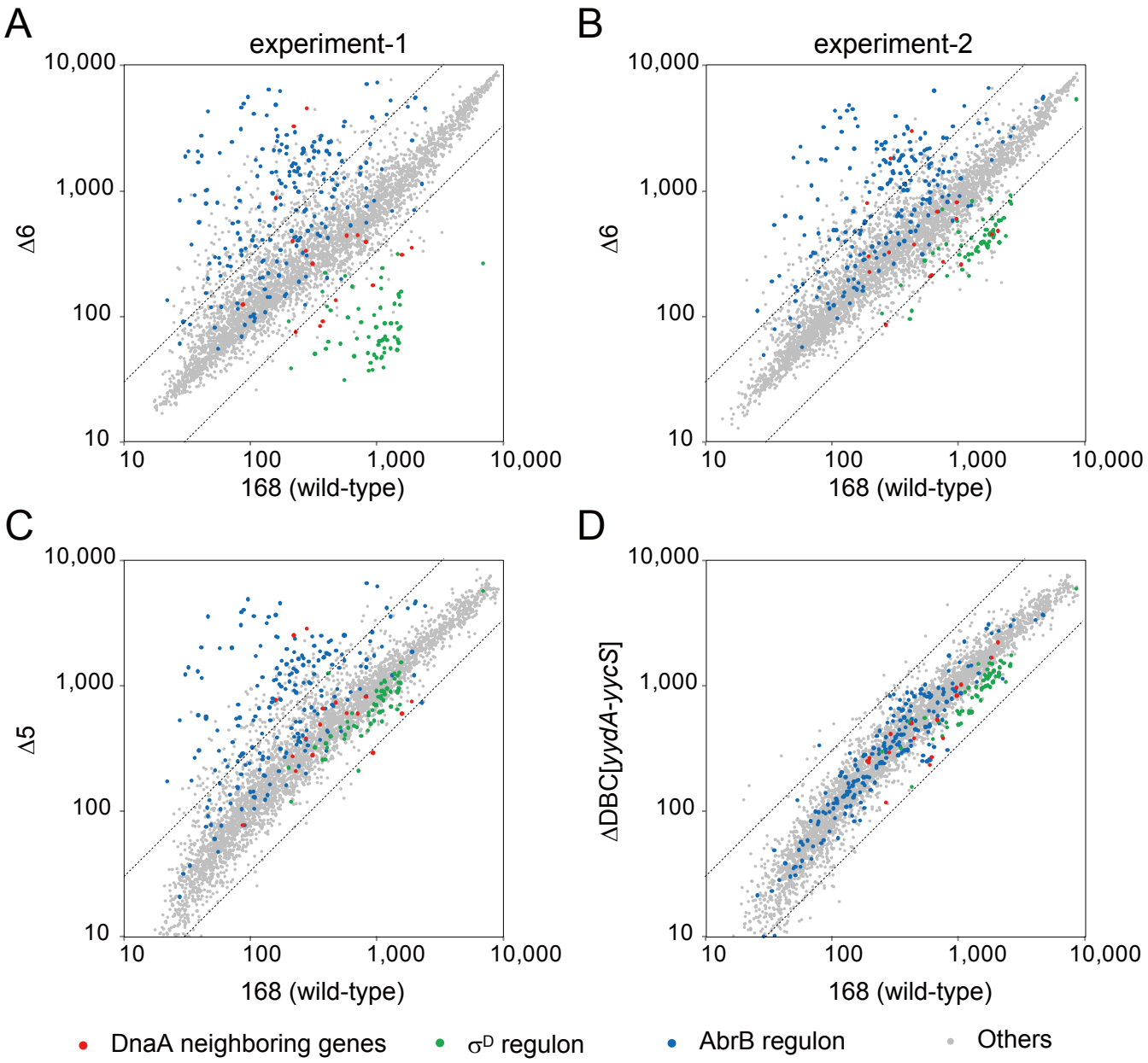
A
experiment-1
Δ6
168 (wild-type)
B
experiment-2
Δ6
168 (wild-type)
C
Δ5
168 (wild-type)
D
ΔDBC[yydA-yycS]
168 (wild-type)
10,000
1,000
100
10
DnaA neighboring genes
σD regulon
AbrB regulon
Others

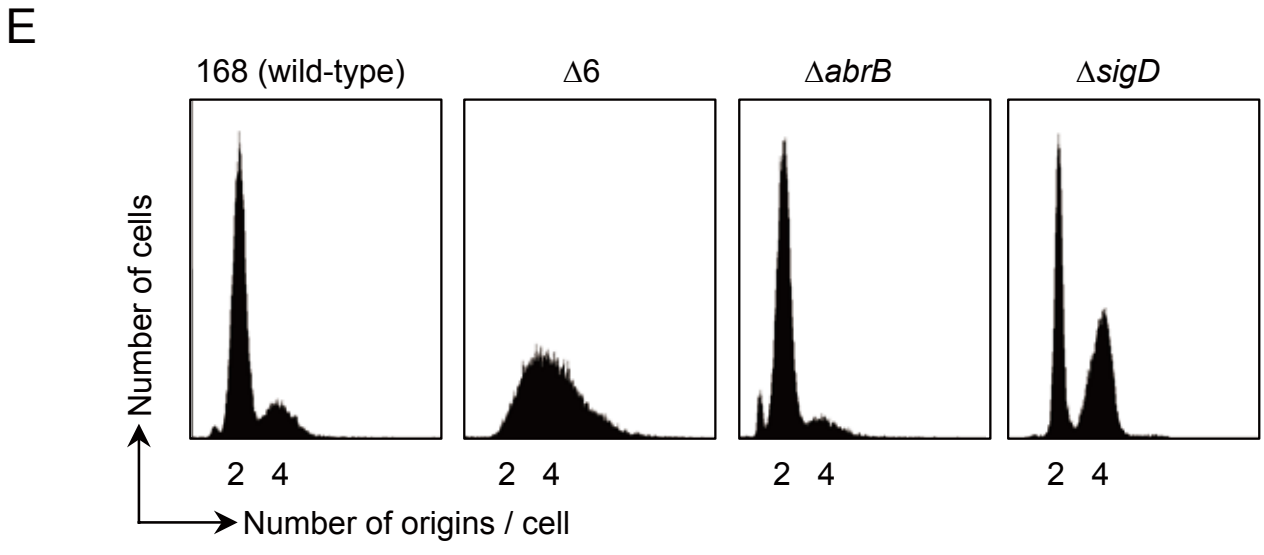
E
168 (wild-type)
Δ6
ΔabrB
ΔsigD
Number of cells
2 4
Number of origins / cell

Fig. S13

A

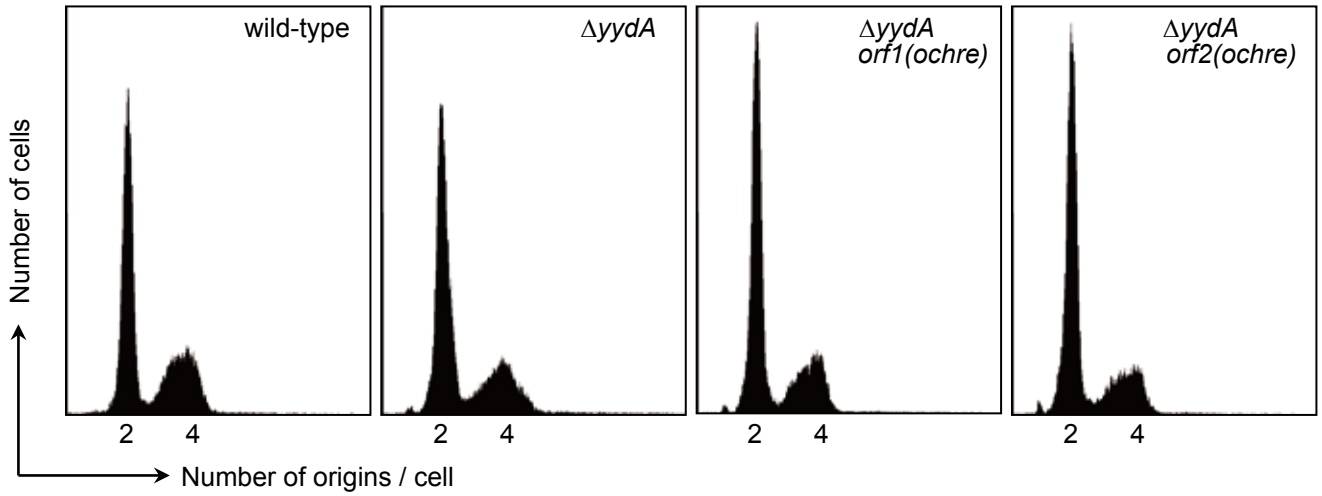
wild-type
ΔyydA
ΔyydA orf1(ochre)
ΔyydA orf2(ochre)
Number of cells
2
4
Number of origins / cell

B

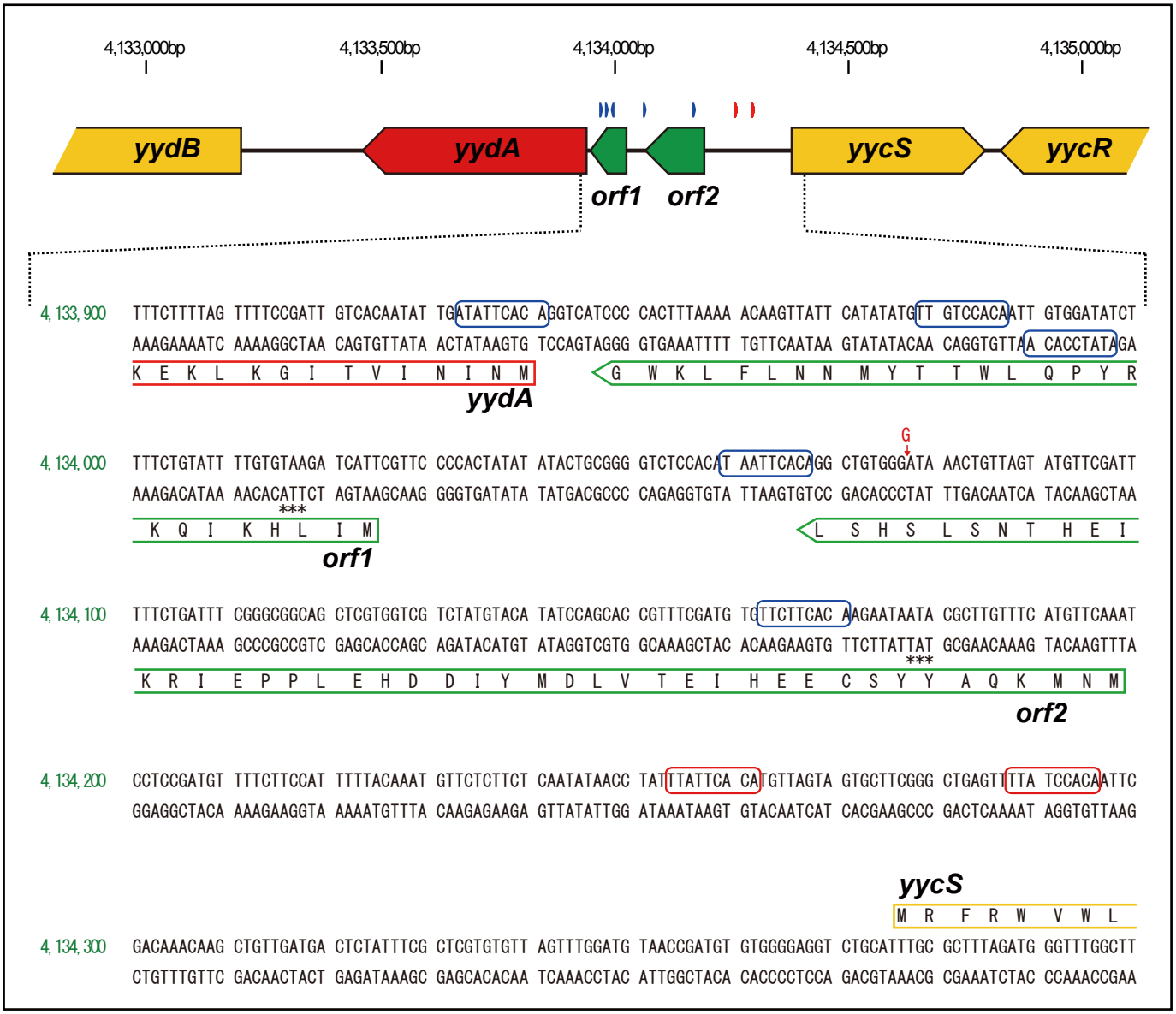
4,133,000bp
4,133,500bp
4,134,000bp
4,134,500bp
4,135,000bp
yydB
yydA
orf1
orf2
yycS
yycR
4, 133, 900
TTTCTTTTAG TTTTCCGATT GTCACAATAT TGATATTCAC AGGTCATCCC CACTTTAAAA ACAAGTTATT CATATATGTT GTCCACAATT GTGGATATCT
AAAGAAAATC AAAAGGCTAA CAGTGTTATA ACTATAAGTG TCCAGTAGGG GTGAAATTTT TGTTCAATAA GTATATACAA CAGGTGTTAA CACCTATAGA
K E K L K G I T V I N I N M
G W K L F L N N M Y T T W L Q P Y R
yydA
4, 134, 000
TTTCTGTATT TTGTGTAAGA TCATTCGTTC CCCACTATAT ATACTGCGGG GTCTCCACAT AATTCACAGG CTGTGGGATA AACTGTTAGT ATGTTCGATT
AAAGACATAA AACACATTCT AGTAAGCAAG GGGTGATATA TATGACGCCC CAGAGGTGTA TTAAGTGTCC GACACCCTAT TTGACAATCA TACAAGCTAA
K Q I K H L I M
L S H S L S N T H E I
orf1
4, 134, 100
TTTCTGATTT CGGGCGGCAG CTCGTGGTCG TCTATGTACA TATCCAGCAC CGTTTCGATG TGTTCTTCAC AAGAATAATA CGCTTGTTTC ATGTTCAAAT
AAAGACTAAA GCCCGCCGTC GAGCACCAGC AGATACATGT ATAGGTCGTG GCAAAGCTAC ACAAGAAGTG TTCTTATTAT GCGAACAAAG TACAAGTTTA
K R I E P P L E H D D I Y M D L V T E I H E E C S Y Y A Q K M N M
orf2
4, 134, 200
CCTCCGATGT TTTCTTCCAT TTTTACAAAT GTTCTCTTCT CAATATAACC TATTTATTCA CATGTTAGTA GTGCTTCGGG CTGAGTTTTA TCCACAATTC
GGAGGCTACA AAAGAAGGTA AAAATGTTTA CAAGAGAAGA GTTATATTGG ATAAATAAGT GTACAATCAT CACGAAGCCC GACTCAAAAT AGGTGTTAAG
yycS
M R F R W V W L
4, 134, 300
GACAAACAAG CTGTTGATGA CTCTATTTCG CTCGTGTGTT AGTTTGGATG TAACCGATGT GTGGGGAGGT CTGCATTTGC GCTTTAGATG GGTTTGGCTT
CTGTTTGTTC GACAACTACT GAGATAAAGC GAGCACACAA TCAAACCTAC ATTGGCTACA CACCCCTCCA GACGTAAACG CGAAATCTAC CCAAACCGAA

Fig. S14

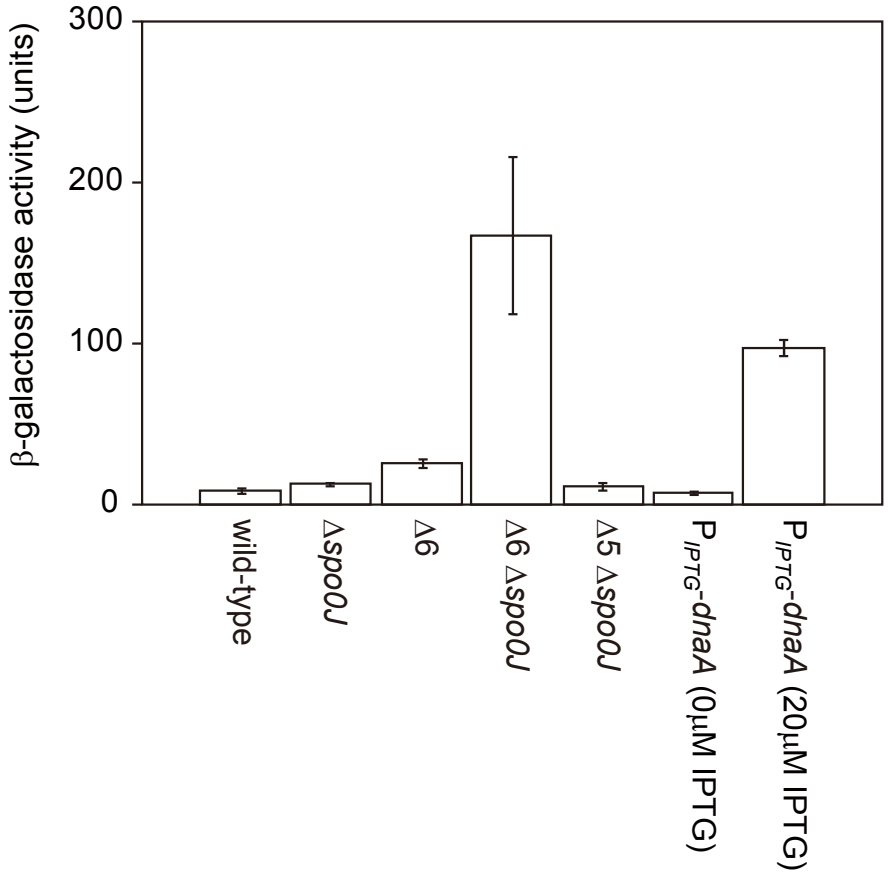
β-galactosidase activity (units)
300
200
100
0
wild-type
Δspo0J
Δ6
Δ6 Δspo0J
Δ5 Δspo0J
P_IPTG-dnaA (0μM IPTG)
P_IPTG-dnaA (20μM IPTG)

Fig. S15

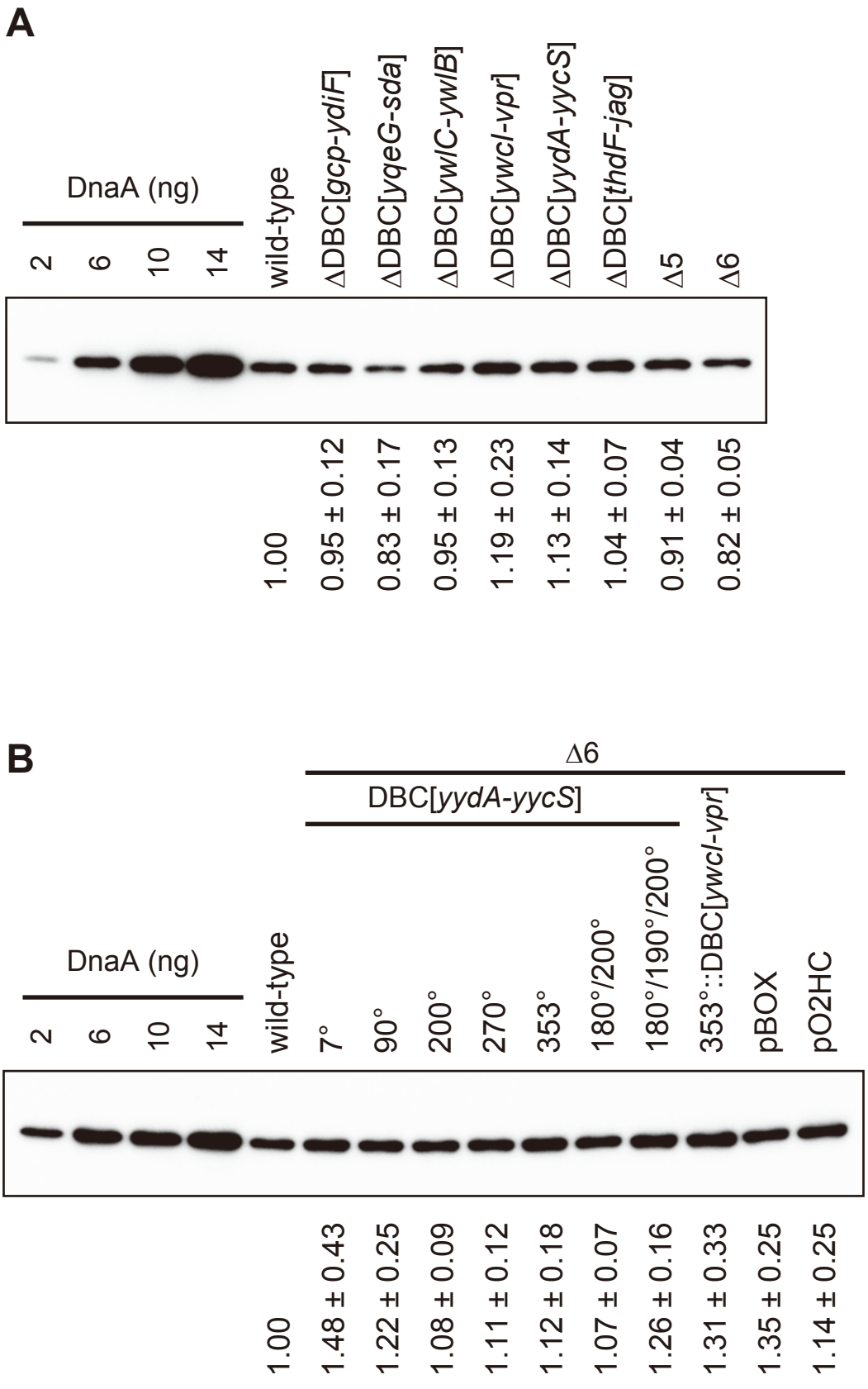
A
DnaA (ng)
2
6
10
14
wild-type
ΔDBC[gcp-ydiF]
ΔDBC[yqeG-sda]
ΔDBC[ywlC-ywlB]
ΔDBC[ywcI-vpr]
ΔDBC[yydA-yycS]
ΔDBC[thdF-jag]
Δ5
Δ6
1.00
0.95 ± 0.12
0.83 ± 0.17
0.95 ± 0.13
1.19 ± 0.23
1.13 ± 0.14
1.04 ± 0.07
0.91 ± 0.04
0.82 ± 0.05
B
Δ6
DBC[yydA-yycS]
DnaA (ng)
2
6
10
14
wild-type
7°
90°
200°
270°
353°
180°/200°
180°/190°/200°
353°::DBC[ywcI-vpr]
pBOX
pO2HC
1.00
1.48 ± 0.43
1.22 ± 0.25
1.08 ± 0.09
1.11 ± 0.12
1.12 ± 0.18
1.07 ± 0.07
1.26 ± 0.16
1.31 ± 0.33
1.35 ± 0.25
1.14 ± 0.25